ASSISTED AND AUTOMATED AERIAL REFUELLING – OVERVIEW OF THE CONDUCTED RESEARCH AT THE GERMAN AEROSPACE CENTER (DLR)

Thomas Jann[1], Nicolas Fezans[1], André Koloschin[1], Sven Olaf Schmidt[1],
Philipp Link[1], Julia Ament[1] & Stefan Krause[1]

[1]German Aerospace Center (DLR), Institute of Flight Systems

Abstract

Air-to-air refuelling has a high strategic and tactical relevance in many military missions, and is one of the most difficult and challenging maneuvers for pilots of military aircraft. Increasing the level of automation is expected to improving the efficiency and safety of air-to-air refuelling operations. Automation is also essential for the aerial refuelling of future unmanned air vehicles. This paper presents an overview of some recent investigations conducted at DLR on the modelling, simulation, and automation of air-to-air refuelling operations with the probe-and-drogue system. Various tanker/receiver pairs were considered: buddy-buddy refuelling between military transport aircraft (similar to A400M), the refuelling of fighters, helicopters, and UAVs by a military transport aircraft. A smart drogue concept (actively stabilised and/or steerable) is also investigated.

Keywords: air-to-air refuelling, modelling, simulation, automation, pilot assistance

Acronyms

AAR Air-to-Air Refuelling
AAS Acceleration Augmentation System
ACP Airload Computation Point
ACT/FHS Active Control Technology / Flying Helicopter Simulator
AVES Air Vehicle Simulator
CFD Computational Fluid Dynamics
CG Center of Gravity
COTS Commercial off-the-shelf
DLC Direct-Lift-Control
DLR German Aerospace Center
DNW-NWB German-Dutch Wind Tunnels - Low Speed Wind Tunnel Braunschweig
DOF Degrees of Freedom
DTC Drogue Tracking Controller
EDA European Defence Agency
F(AI)²R Future Air-to-Air Refuelling
FCU Flight Control Unit
FMTA Future Military Transport Aircraft
FoV Field of View
FPA Flight Path Angle
FPV Flight Path Vector
GFA Generic Fighter Aircraft
GHM Generic Helicopter Model

GNSS Global Navigation Satellite System
HAAR Helicopter AAR
HMD Helmet-Mounted Display
HOTAS Hands On Throttle and Stick
HTA Hierarchical Task Analysis
HUD Head-Up Display
IMU Inertial Measurement Unit
LiDAR Light Detection and Ranging
MARS-FIT Military Air Vehicle Simulator - Fast Integration Testbed
ND Navigation Display
NIR Near-Infrared
PFD Primary Flight Display
PnP Perspective-n-Point
PTC Position Tracking Controller
RANS Reynolds-averaged Navier-Stokes
RTIG Real-Time Image Generator
SA Situational Awareness
SAR Situational Awareness Requirements
SFR Simulation Fidelity Rating
SHC Speed Hold Controller
TRL Technology Readiness Level
UAV Unmanned Aerial Vehicle

1. Introduction

Air-to-air refuelling (AAR) has a high strategic and tactical relevance in many military missions, and is one of the most difficult and challenging maneuvers for pilots of military aircraft. Increasing the level of automation is expected to improving the efficiency and safety of air-to-air refuelling operations. Automation is also essential for the aerial refuelling of future unmanned air vehicles.

DLR (the German Aerospace Center) recently concluded a four-year project called F(AI)^{2}R (Future Air-to-Air Refuelling, 2019-2023) aiming at developing methods for the assisted and automated refuelling of fixed wing and rotary wing aircraft with the probe-and-drogue system. Modelling and simulation have been essential parts of the research, required to understand the dynamics of the process and build up a test environment for automation systems with – and eventually without – the pilot in the loop. This included the development of flight-dynamical models for the involved aircraft, the investigation of the aerodynamic interference between both aircraft in formation flight, the development of a model for the hose-and-drogue refuelling system, and its real-time implementation into the DLR simulator facilities AVES and MARS-FIT.

The new automation methods particularly address the receiver aircraft, in order to extend its capabilities with respect to the automatic approach, coupling and formation keeping for AAR. The spectrum goes from pilot assistance systems, over semi-automatic functions to fully automated air-to-air refuelling maneuvers. As a new concept also the active aerodynamic control of the refuelling drogue has been addressed and investigated.

The paper gives an overview about the developments and results achieved within the F(AI)^{2}R project. It is organised around three main parts: the modelling of the various platforms, their coupling, and specific refuelling systems are presented in section 2. Section 3 presents the simulation environments developed and used and finally section 4 presents the various pilot assistance and automation concepts developed during the F(AI)^{2}R project.

2. Modelling

In contrast to a typical flight simulation, which incorporates only one air vehicle, air-to-air refuelling requires the simulation of two aircraft, the tanker and the receiver. As both aircraft interact through aerodynamic effects and through the refuelling system, the overall simulation is not a simple aggregation of two individual aircraft simulations. The modelling work in F(AI)^{2}R has built upon prior work, e.g. from the project LUBETA [1; 2], in which a buddy-buddy refuelling simulation between two A400M-like configurations, named Future Military Transport Aircraft (FMTA), so as tanker and also as receiver, was developed. In F(AI)^{2}R the models and simulations have been significantly extended towards the aerial refuelling of helicopters and fighters, while using the FMTA still as model for the tanker. The FMTA-FMTA simulation was also significantly improved.

2.1 Considered Aircraft Models

To be able to perform research on military aircraft and missions with little to no intellectual property or confidentiality restrictions, DLR has defined a series of generic aircraft configurations which are representative of the different types of existing or planned vehicles and developed flight dynamics models of these configurations. They are presented in the following sections.

2.1.1 FMTA: Future Military Transport Aircraft (Manned Tanker and Receiver)

The Future Military Transport Aircraft or FMTA is the configuration with the longest history. It was defined about 20 years ago and largely inspired by the Airbus A400M, which was being designed at the time (hence the adjective *future* in its name, which has not been changed since). Its basic dimensions, mass, capabilities, etc. are similar to the A400M, but none of the details (slightly different geometry, different airfoils, different high-lift system, etc.) are identical to the A400M. In this condition the FMTA model is widely generic, but still sufficiently representative and therefore adequate for DLR research activities.

The flight dynamics model of FMTA has been initially developed as a limited test case for a model-based performance evaluation tool [3] and continuously used, further developed, and extended since

2

[4–8]. Around 2015/2016, FMTA was ported from a former flight simulator to the DLR AVES's simulator[1] [1; 2; 9; 10].

When refuelling with the probe and drogue system, the most challenging flying task in on the receiver' side, so when simulating the refuelling of one FMTA with another FMTA, the focus lies on the receiver and the simulator cockpit is used to fly the receiver (cf. details in section 3). The change of weight and balance properties due to the fuel being transferred from the tanker to the receiver is accounted for both for the tanker and the receiver. RANS-CFD computations, in which the propellers were modelled as actuator disks, were used to precisely model the impact of the propeller slipstream on the wing aerodynamics as well as the nonlinear characteristics of the spoilers for the considered FMTA-FMTA refuelling flight point (260 kts CAS, 20,000 ft).

For the refuelling of relatively slow vehicles (e.g., helicopters), a high-lift system was designed by the colleagues of the DLR Institute of Aerodynamics and Flow Technology, who also computed the wake behind the tanker computed also for a wide range of speeds/angle of attack and flap settings (cf. section 2.2 and [11; 12]). Three refuelling points are available: the centerline and a wing pod under each wing. The probe of FMTA (as receiver) is not retractable and extends from the top-left of the cockpit, and is slightly tilted downwards and to the right. For the pilot seated left, the probe tip is slightly above and left of the head-up display top-left corner, so well in his/her field-of-view.

2.1.2 GFA: Generic Fighter Aircraft

The Generic Fighter Aircraft is originally based on the aerodynamic dataset of the F-16 published in [13]. It exhibits the classic control surfaces aileron, elevator and rudder, as well as leading edge flaps and speed brakes. As the F-16 is by default refuelled via the Boom Receptacle a refuelling probe was added to the model. Certain modifications have been carried out on the aircraft model, in order to make it more representative of a modern fighter aircraft. This includes a modification of the engine dynamics, as well as a change in drag coefficients to allow simulating the behaviour of a configuration with external stores. Finally, a new flight control system was designed, consequently removing the similarity to the F-16 and resulting in a model of a generic fighter.

2.1.3 GHM: Generic Helicopter Model

The real-time helicopter simulation in AVES is based on DLR's 2Simulate HeliWorX modelling suite, which incorporates a non-linear implementation of a helicopter model [14]. Initially derived from a Bo 105 model utilizing blade element theory, the HeliWorX suite was further developed to represent the dynamics of DLR's research rotorcraft Active Control Technology / Flying Helicopter Simulator (ACT/FHS). The development involved integrating a real-time interference model to replicate local aerodynamic phenomena, such as those encountered when flying through the wake of wind turbines, ships, or aircraft. Leveraging this extended version of the HeliWorX suite, a Generic Helicopter Model (GHM) was introduced and configured to show dynamics similar to a medium lift cargo helicopter (e.g. CH-53). Upon completion of the configuration process, a three-axis stability augmentation system was manually fine-tuned. The GHM is intended to be utilized for various studies in DLR's projects regarding air-to-air refuelling. More information can be found in [11].

2.2 Aerodynamic Interaction and Turbulence

During the refuelling process, both aircraft are flying behind each other in close formation, potentially interfering with each other aerodynamically, depending on their exact relative positions.

The tanker wake is the tanker's influence on the flow field in the area behind the aircraft, including downwash, vortices and disturbances coming from wings, fuselage, control surfaces and engines. The induced wind acts on the hose and drogue system and on the receiver aircraft. It changes depending on the flight conditions and position relative to the tanker. To incorporate this effect into the simulation, quasi-steady CFD flow fields have been pre-calculated and stored into look-up tables that were used by the model.

---

[1]https://www.dlr.de/en/research-and-transfer/research-infrastructure/
air-vehicle-simulator

The receiver also creates the so-called bow wave that changes the airflow around its nose section. At the distances at which the refuelling with the probe-and-drogue system are performed, the bow wave's influence on the tanker is only marginal. The bow wave primarily affects the hose-and-drogue system: when the receiver approximates the drogue, the changed airflow typically pushes the drogue laterally and vertically, away from the receiver bow, and so away from the probe. To establish contact with the drogue, the receiver pilot tries to predict this change of the drogue position and adjusts the very last part of receiver trajectory in anticipation of the drogue reaction to the bow wave.

2.2.1 Tanker Wake

To refuel, tanker and receiver have to fly at the same altitude ($\pm$ the vertical offset of the drogue which hangs slightly below the tanker) and speed. During the F(AI)^{2}R project, two flight points have been considered. One flight point is in the medium-high-speed region at 260 KCAS and 20,000 ft for jet and transport aircraft refuelling, and the other is in the low-speed region at 115 KCAS at 7,000 ft for helicopter air-to-air refuelling. In the latter case, the tanker is flying with extended flaps. For both flight points a series of flow fields have been computed with CFD for different angles of attack, airspeed and flap configurations. Based on the generated data, adjustments for varying tanker weights and flap settings can be performed by interpolating between the computed flow fields.

For the CFD computation of the tanker wake, the flow solver DLR TAU was used, and applied to an hybrid unstructured grid around the FMTA geometry. To reduce numerical dissipation of the created flow vortices from the tanker, the volume mesh was refined in the relevant areas, where receiver maneuvering and refuelling is expected [1; 12; 11]. TAU performs a Reynolds-averaged Navier-Stokes (RANS)-CFD simulation using the Spalart-Allmaras turbulence model. The tanker wake flow is dominated by the wing downwash, the wing tip vortices, and the inner and outer propeller slip streams. Furthermore, a fuselage wake flow and a wake flow around the wing pods are present. For the high-lift configuration at low speed, additional vortices are created by the extended high-lift flaps.

The tanker wake was implemented into the real-time simulation environment using lookup-tables with equidistant mesh. Free airstream and global winds are separately considered and superimposed with the airflow of the tanker wake flow field for force calculation. Hence, airstream is subtracted from the CFD solution yielding the actual interference of the tanker wake on the airflow. The flow field is stored within a three-dimensional lookup table, its origin matches tanker FMTA's reference point and it sticks to the tanker's translational movements.
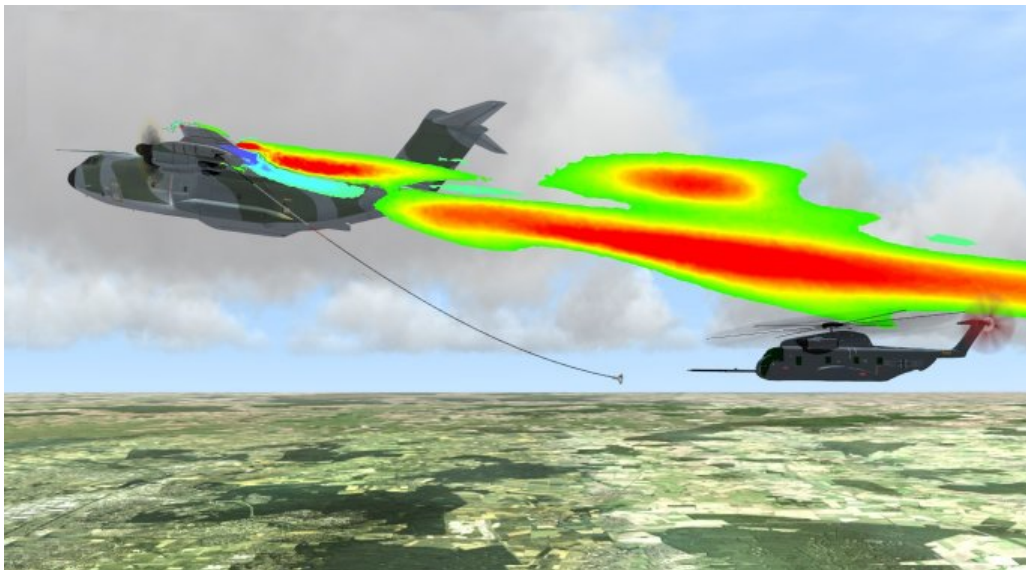
Figure 1 – Simulation of GHM behind FMTA's 120 ft hose with CFD-computed tanker wake

Fig. 1 shows a visualisation of the vortex topology of the tanker's wake flow, where the vorticity component orthogonal to the y-z plane ω_x is overlaid to the 3D visualisation of FMTA and GHM. Because of issues during A400M HAAR certification described in [15], the standard 80 ft refuelling

hose was extended to a 120 ft hose. Both hose lengths were considered for the simulated HAAR scenario and investigated in [11]. The figure illustrates the GHM in astern position resulting from the 120 ft hose and provides an impression of the potential impact on the receiver by the tanker's propeller downwash in a more forward and upward astern position resulting from the 80 ft hose.

2.2.2 Bow Wave

The impact of the bow wave on the drogue depends on the dimension and shape of the fuselage front section, and the distance of the probe tip or probe length. For fighter and transport aircraft refuelling the bow wave needs to be considered. In contrast, because of the long probe shaft, the effect is usually neglected for helicopter refuelling.

The flow field for the bow wave of the FMTA was obtained from the same CFD computations of the tanker wakes. For this purpose, the volume mesh was also refined around the front section and the probe, and then extracted into a lookup table for real-time simulations [1].

For the adaptation to fighter aircraft, new bow wave flow fields for the fighter front section have been computed and implemented using a potential aerodynamic method [16]. This results in a simple approximation of the flow condition without requiring CFD data, while still exhibiting the characteristics of the flow, e.g. the dependency on the airspeed.

2.2.3 Atmospheric Turbulence

In addition to the aerodynamic interaction between the two aircraft and the other objects of the refuelling system, the atmospheric turbulence is another very important influencing factor in an air-to-air refuelling scenario. Because of a few unique requirements, a new model for atmospheric turbulence has been developed with the purpose of being representative specifically for the simulation of air-to-air refuelling. Generally, an important property of atmospheric turbulence is its stochastic nature which can be modeled based on random number generators and the turbulence power spectral density (PSD). Because the air-to-air refuelling simulation includes two aircraft in close formation and additional objects of the refuelling system, the corresponding turbulence velocities should be correlated. A limited consistency can be obtained by defining a virtual point and by using transport delays (cf. [2, section 2.3.6]), but this approach is far from being optimal, especially when refuelling with wing pods as the tanker and the receiver are flying parallel trajectories and are not behind each other anymore. Consequently, ways to improve the turbulence model for such formations were investigated.

The new turbulence model needed to reproduce the stochastic nature of real turbulence but model the more or less strong and potentially delayed correlation between the wind speed encountered by objects that are in close proximity to each other, depending on their relative positions. Another important requirement was to simulate variations of the turbulence magnitude. In reality, the magnitude of atmospheric turbulence is not constant - even for relatively short time frames - but varies between slightly weaker and slightly stronger turbulence. Apart from a better immersion for pilots as the turbulence does not feel too regular anymore, this effect is particularly important for air-to-air refuelling. The pilot of the receiver aircraft typically observes the movement of the refuelling drogue due to the turbulence and often waits for a short moment with lower turbulence and thus a smaller drogue oscillation before attempting to establish contact with the drogue. Similar to the stochastic behaviour of the turbulence itself, these variations of the turbulence magnitude need to be sufficiently random to remain unpredictable for the pilot.

A new turbulence model fulfilling these requirements has been developed. The basic principle of this model is the calculation of the wind speed components using a fairly complex analytical function, which guarantees that the generated wind speeds produce overall the right spectrum in all directions, and that the overall function also consistently provides the same wind vector when called several times for the same location. This provides a spatial wind field function that can be evaluated globally without having to store the wind field itself. Otherwise, with the distances covered in a refuelling scenario and the point density needed to represent the highest frequencies of the turbulence field, the amount of memory that would be needed to store the wind field as a lookup table would be enormous. Figure 2 shows an example how the generated turbulence field can look like with some
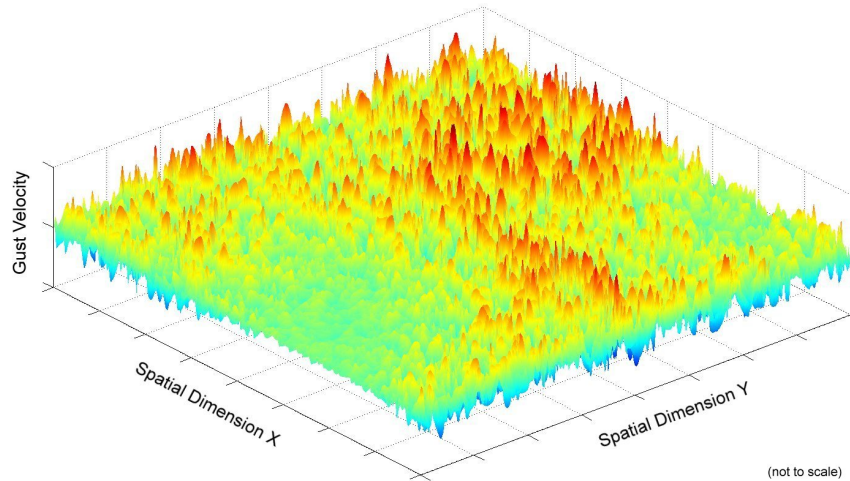
Figure 2 – Schematic example section of a turbulence wind field with a varying magnitude

areas of lower and some areas of higher turbulence magnitude. It has been integrated into the software framework for the aerodynamic interaction that will be explained in the next section. The details of this new turbulence model will be published in the near future in a dedicated paper.

2.2.4 Aerodynamic Interaction

For the implementation of the aerodynamic interaction, a software framework was developed, which manages the superposition of flow fields, the transformation airflow vectors into arbitrary coordinate systems, and the computation of forces and moments due to in-homogeneous airflow across the receiver geometry. The simulation mechanism used by this framework to interact the simulation of the formation (mostly implemented with Simulink and from which its code is generated) is presented in [10]. For the computation of the aerodynamic interaction two main model parts are needed: (1) the wind fields resulting from the different objects and their aerodynamic properties and (2) a model of how the local flow impacts the aerodynamic forces and moments of the objects/components that encounter them. For the implementation of the wind fields, data can be extracted from CFD computations and implemented as lookup tables. Turbulence but also low-order potential methods (e.g. for the bow wave) can be superimposed. Each of the wind field may be attached to (and so move with) different objects contained in the simulation, e.g. tanker, receiver, drogue, or even fixed with respect to the Earth. They may also be expressed using locally defined coordinate systems

For the modelling of their impact on the objects, usually some form of discretisation of the object geometry is needed, e.g. decomposing the wings, fuselage, and empennage in strips or panels. When computation the aerodynamic forces and moments for them, usually the local flow for specific points of the geometry is needed (e.g. at the control points of each panel to compute the right hand side vector or Neumann boundary conditions of the problem). This means that the wind data for many points in space and their projections in different directions need to be computed. This involves many coordinate transformations to convert the position of each point of interest in the local coordinates of each wind field. A relative kinematics components allows users to define these requests with a rather high-level and declarative syntax, while taking care of applying the right transformations behind the scenes. This last component is non-functional, in the sense of not constituting a physical model and not impacting the computations made, but drastically eases the management of many coordinate systems, wind field sources, etc. and reduces the risk for errors. As FMTA has a fairly simple wing geometry (trapeze wing with typical aspect ratio and with linear twist distribution along the wing span) a simple vortex ladder method with a Prandtl-Glauert Mach number correction is used both for the tanker and the receiver aircraft (typical Mach number for FMTA-FMTA refuelling is 0.6). As explained in [10], the method is only applied to the inhomogeneous part of the wind field. The *locally*

averaged relative wind is sent to the basis aerodynamic model of the FMTA and the aerodynamic interaction is only a correction to the basis aerodynamic model that is active only in the presence of inhomogeneous flow over the airframe.

The calculation of the aerodynamic interaction for the GFA follows the approach used for the FMTA, taking into consideration the different geometry of the receiver. The final result reflects the inhomogeneous flow conditions at different relative positions to the tanker and was finally validated in simulator tests with experienced fighter pilots.

For the influence of the tanker wake on the GHM the approach described in [17] was followed, utilizing Airload Computation Points (ACP) that are distributed over the main rotor as well as the refuelling hose's lumped masses and the drogue. The illustration in Fig. 3 shows the ten defined ACP per rotor blade and one additional ACP as a reference that is located on the rotor hub. Based on each ACP's current position relative to the origin of the flow field, the local air flow velocities are linearly interpolated using the flow field lookup table.
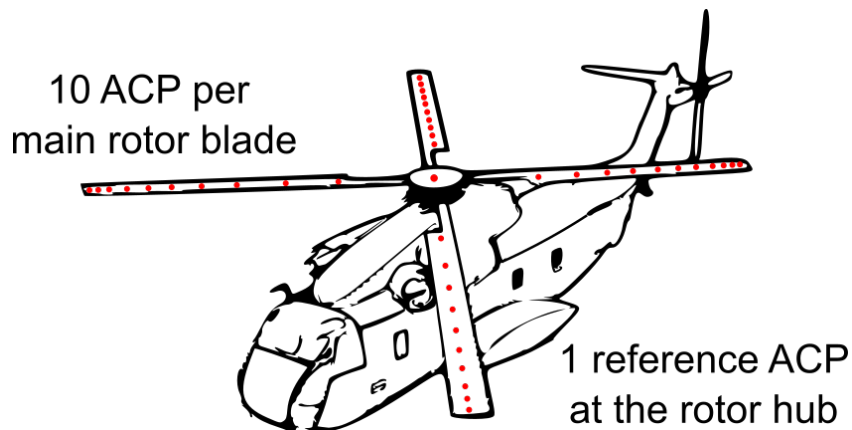
Figure 3 – Distribution of ACP over the rotorcraft receiver GHM [11]

The distribution and number of ACPs on the main rotor is considered sufficient for piloted simulation [17]. However, some HAAR experienced pilots mentioned a lack of dynamic characteristics, so the quasi-steady tanker wake is supported by a scaled Dryden turbulence model adding an unsteady portion to the airflow [18].

2.3 Refuelling System

The model considers hose-and-drogue refuelling from the tanker centerline or from one of the wing pods. For the hose, a physically-deduced multi-body lumped-mass model with up to 50 coupled point masses was developed. The masses are concentrated in the nodes that are connected by mass-less spring-damper elements. The longitudinal elasticity of the hose is modelled using a translational spring-damper system within each segment, and its bending stiffness is modelled with a rotational spring-damper system between the segments (i.e. at the masses locations). Having force-moment couplings instead of kinematic constrains between the bodies of the model facilitates structural changes the model and the separation, addition or removal of bodies during the simulation. This feature is used here for changing the hose length by adding or eliminating segments and nodes during the reeling-out or reeling-in process. The nodes are either located at the hose attachment point inside the hose drum unit, or they are released and form part of the reeled-out portion of the hose. In the present model, a drag coefficient is associated to each of the nodes (respectively point masses). At each node, the local airflow generates a local force which is injected into the equations of motions of the corresponding masses. The local airflow is provided by the methods described above, such that the aerodynamic interaction of the moving hose nodes within the tanker wake, bow wave and turbulence is fully included in the model.

The drogue is modelled as axis-symmetric rigid body with 6 degrees of freedom and corresponding aerodynamic drag characteristics. Its mass is provided as input parameter by the user, whereas moments of inertia and center of gravity are derived from it considering its shape. The drag force

acts on the center of pressure, which is located downstream of its CG. Within the drogue model there are two geometrically relevant points: the attachment point for the hose, and the coupling point for the probe. The attachment point is treated like a node between the last hose segment and the drogue body, except it is mass-less, since mass and aerodynamics are created by the rigidly connected drogue. The coupling point is located in or close to the tip of the inner cone geometry of the drogue. When probe and drogue are coupled, probe tip and coupling point coincide and the drogue is aligned with respect to the probe.

The receiver probe geometry is defined within the refuelling model to allow the implementation of a contact model between probe and drogue. This contact model accounts for the conical inner and outer geometry of the drogue basket and determines the proper reaction force in case of collision between the probe and the inner or outer drogue surfaces. The reaction force is obtained by the penetration distance and a visco-elastic spring-damper model. The behaviour of the system changes between the non-coupled state, for which the contact model is required, and the coupled state where the drogue is firmly attached to the probe, whereby the transitions between the different states are managed using a state machine. A coupling is successful, i.e. the transition from the uncoupled to the coupled state is made, if the probe tip enters the coupling zone inside the basket and transfers at least some pre-defined minimum momentum to the drogue. Upon coupling, the drogue states are progressively set to the position and attitude of the probe tip, with the result that eventually the drogue follows every motion of the probe. Separation (i.e. transition from the coupled to the uncoupled state) occurs as soon the traction force in the connected hose segment exceeds a given threshold.

Figure 4 – Simulated centerline refuelling with two FMTA

The length of the flexible hose is controlled by the hose drum, which is located inside the wing pods of the tanker aircraft, or in the rear fuselage for centerline refuelling. The hose drum contains the drum including driving gear motor and corresponding controllers, and the fuel pumps and valves that control the fuel flow through the hose. In the model, the hose drum subsystem is mainly responsible for controlling the hose extraction and retraction, whereas the fuel management is the task of a separate subsystem. The incorporated tension controller allows the simulated refuelling system to react realistically when the receiver probe gets in contact with the drogue, and moves forward to enter the refuelling zone. A model of the refuelling logic and fuel management controls fuel flow and signal lights on the tanker indicating the refuelling status to the receiver pilot.

To control the refuelling system within the simulation, for example to send commands for trailing or rewinding the hose, and to display the status, a graphical user interface (GUI) named 'AAR Panel' was developed and integrated with the overall simulation. The functions and layout were inspired

from the refuelling control pages in the A400M cockpit, such that this panel will be familiar to A400M pilots. Some modifications were made for the need of the project and to ease its handling and testing in the simulator. For instance, options to adjust the maximum fuel flow or to change some drogue characteristics were added.

3. Full Simulation

The full simulation, which combines the models for tanker, receiver, refuelling system and aero-dynamic interaction, serves as basis for the test of new and specialised control algorithms for the automated aerial refuelling. Due to differences in the requirements for the simulation of the different tanker-receiver pairs, each full simulation has its own characteristics, even if whenever possible and meaningful modules have been shared and synergies exploited. The simulations for FMTA and helicopter were then transferred into the corresponding DLR simulators AVES (Air Vehicle Simulator) [9; 1; 11] to conduct simulator tests with pilots-in-the-loop. For the simulation of fighter refuelling, the new simulator MARS-FIT (Military Air Vehicle Simulator - Fast Integration Testbed) was developed, built and used within the project [19].

Figure 5 – Air Vehicle Simulator (AVES) at DLR Braunschweig

The Air Vehicle Simulator (AVES) facility [9], depicted in Fig. 5, is DLR's research flight simulation infrastructure located in Braunschweig, Germany. It comprises the following four modules: an Airbus Helicopter EC135 cockpit, an Airbus A320 cockpit, a single aisle passenger cabin, and the cockpit of a Dassault Falcon 2000LX. These modules can be interchanged via a roll-on/roll-off system to be mounted either on a full-sized six-degree-of-freedom (DOF) hexapod motion platform or on one of two fixed-base platforms. All platforms have a broad horizontal Field of View (FoV) spanning 240° and a vertical FoV ranging from –55° to 40°. The simulator's image generation is powered by DLR's in-house real-time image generator (RTIG) software, utilizing the OpenGL render engine. This open-source platform facilitates seamless integration of new features, i.e. refuelling equipment. Although several components adhere to commercial training simulator standards, it's crucial to note that AVES is primarily a research simulation facility and does not intend to meet EASA FSTD standards.

3.1 FMTA-FMTA Refuelling Simulation

In the FMTA-FMTA case, the simulation software consists of an integrated model with the entire flight physics being integrated and solved together. This eases the implementation of a coupling between all parts of the model even within minor steps of multi-stage numerical integration methods. For easier maintenance, the most of the rest of the infrastructure is identical between the case where two FMTA are simulated and the case where only FMTA is simulated. As shown in the diagram of Figure 6, most modules are duplicated in the infrastructure and only treat the information of one of the two FMTA. The two main exceptions are the Instructor and Operator Station, which controls the overall architecture and the visualisation software.
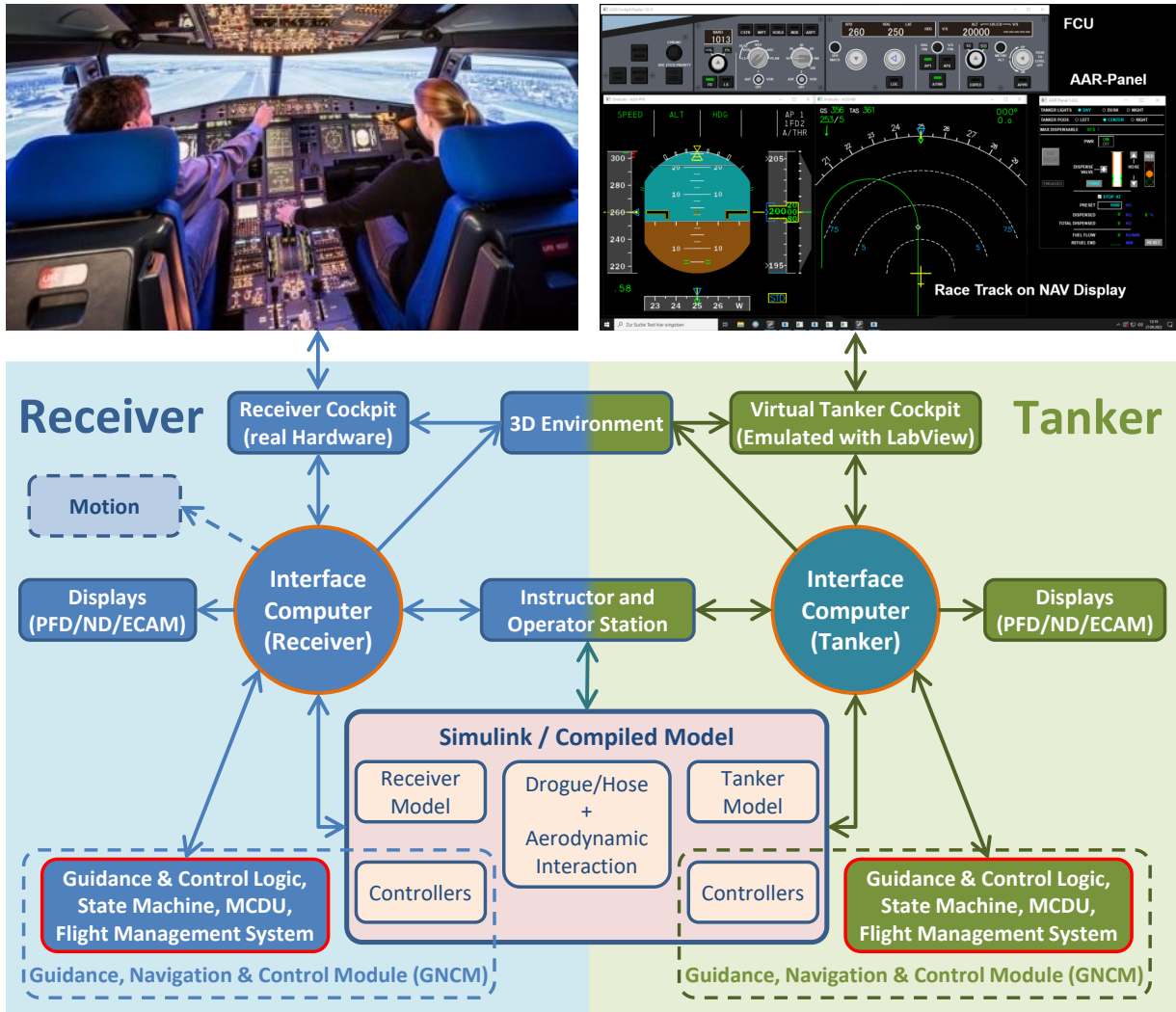
Figure 6 – Simulation Architecture in the FMTA-FMTA Case

The receiver is controlled by the Airbus A320 Cockpit, whereas the tanker is operated via a virtual tanker control station. This station is a virtualised version of a cockpit and mainly consists of a primary flight display (PFD), a navigation display (ND), an emulated flight control unit (FCU), an AAR Panel, and, when connected, a standard gaming joystick. The tanker operator station is usually deployed on the second operator station, which is located in the aft part of the cockpit module, behind the co-pilot seat and separated by a wall (no direct view between pilot seats and the tanker operator station).

3.2 Helicopter Refuelling Simulation

The EC135 cockpit is utilised for helicopter simulations and mimics the interior layout of DLR's research helicopter, Active Control Technology / Flying Helicopter Simulator (ACT/FHS). Equipped with a fly-by-wire/fly-by-light flight control system and various research measurement equipment, this modified EC135 differs significantly from standard operational variants of the aircraft type. Besides

standard EC135 inceptors, the rotorcraft and simulator cockpit includes quickly applicable sidesticks and experimental displays with touchscreen capability on the pilot's side. Fig. 7 shows the view from the AVES cockpit during the approach to formation.

Figure 7 – Cockpit view of the HAAR scenario in AVES [11]

In the AVES test facility, the 3D model of FMTA is projected into the external visual environment. However, due to constraints related to the small simulation step size used for the rotor aerodynamics (1 ms), the tanker (FMTA) motion is represented by a simple point mass moving with a constant heading, altitude, and speed. The full FMTA model is presently too complex for real-time simulation with 1 ms step size. Solutions allowing the coupling of a full FMTA model (6-dof plus systems, flight control system etc.) with GHM might be investigated in the future. To enable realistic contact establishment within the scenario, the multi-body refuelling system, described in section 2.3, was implemented into the helicopter air-to-ait refuelling (HAAR) real-time simulation environment described in [11]. Standard as well as HAAR-specific parameter sets for different overall hose lengths can be found in [12].

Further investigations using the HAAR simulation environment require basic similarity of the pilot's behavior compared to real flight conditions. This was tested with regard to the pilot's control and gaze behavior during the contact and refuelling phase up to the disconnect [18]. The resulting simulation fidelity forms the basis for the validity of further objective measurements. Statements about the simulation's fidelity were made by HAAR experienced pilots using a combination of the Simulation Fidelity Rating (SFR) Scale as well as pre and post trial pilot questionnaires. SFR utilises pilot self-assessment in form of assessing the extent to which training in a simulator can be translated to real-flight scenarios [20]. The simulation of HAAR achieved a good simulation fidelity level 2: 'Simulation's fidelity warrants improvement but limited transfer of training for the selected task is attainable and additional training is required for operational performance'. With regard to the generic character of the simulation, not having to comply to demands expected of a specific training simulation, this level of fidelity is acceptable. As soon as flight test data is available, further verification will be pursued.

3.3 Fighter Refuelling Simulation

In the scope of the project F(AI)^{2}R the new fighter specific fixed-base simulator MARS-FIT (Military Air Vehicle Simulator – Fast Integration Testbed) was built up. It is depicted in Fig. 8. It is based around a decommissioned ejection seat which leads to a high degree of pilot immersion. The classical control elements i.e. force-feedback sidestick, throttle and force-feedback pedals are used as inputs to the simulator. Additionally, multiple buttons and switches are included following the HOTAS concept and allowing the pilot the control of the aircraft, especially for activation of certain automatic control modes. Five 65" monitors provide a horizontal field of view of approximately 120° and a vertical field of view of 38° to the pilot, depicting the view outside the cockpit. This large horizontal field of view is considered necessary for AAR simulation, so that all visual references are visible [21]. The whole simulation including the simulation framework, as well as the visualisation is based on DLR in-house designed software. Additionally, an operator station was set up, to control the simulator setup, as well as to allow live observation of the simulation data. [19]

Figure 8 – Military Air Vehicle Simulator - Fast Integration Testbed (MARS-FIT) at DLR in Manching

In order to validate the whole simulator setup an extensive simulator test campaign was carried out with test pilots of the German air force. After some iterations the whole simulation – including the simulator periphery, i.e. input devices and displays - was rated as representative for a real air-to-air refuelling and the generic fighter aircraft as central point of the simulation was also assessed as representative for a modern fighter aircraft and showing good handling qualities.

4. Automation and Pilot Assistance

Several concepts for automated and assisted air-to-air refuelling have been developed, implemented and evaluated in the simulator. The main focus has been the development of solutions for facilitating the docking process for the receiver pilot. This maneuver represents the most difficult part of the refuelling process, and requires precise relative positioning between receiver and tanker, in particular between probe and drogue. Presently, all methods presuppose a pilot in the loop, who is capable to control the receiver and engage/disengage the automation. For the future, however, also the full automation of the whole refuelling process with all phases, will be considered.

Within the scope of the F(AI)^{2}R project, the word *assistance* was used for concepts that require the pilot to actively control the aircraft with e.g. the control stick. These concepts include pilot assistance by providing additional feedback by e.g. new display information but also include pilot assistance by modifying the flight control laws for this task. In contrast to that, concepts that move the role of

the pilot to a monitoring task while the autopilot is controlling the aircraft have been categorised as *automation*.

4.1 Pilot Assistance

4.1.1 Pilot Assistance by providing additional visual feedback

Eye-tracking investigations within the F(AI)^{2}R project revealed that the docking process is an almost complete eyes-out maneuver, which requires the pilot's full attention on tanker and drogue. During the transition from astern position to contact, and further to the refuelling zone, the pilot keeps his sight fully on the scenery and almost ignores the display on the head-down instruments panel.

In designing assistance systems for air-to-air refuelling in the F(AI)^{2}R project, the situational awareness (SA) of fighter pilots was examined during this demanding maneuver. The assessment emphasised SA's vital role in the success of the refuelling process and offered insights into the effectiveness of the newly developed assistance systems. According to Endsley, SA encompasses "the perception of the elements in the environment within a volume of time and space, the comprehension of their meaning, and the projection of their status in the near future." [22] Based on this definition the study examines air-to-air refuelling using probe-and-drogue equipment from the receiver's perspective, aiming to create an assistance system that enhances pilot SA. This aims to improve performance and lower pilot workload during the refuelling process during the transition from astern position to contact, and further to the refuelling zone where the pilot keeps his sight fully on the scenery and almost ignores the display on the head-down instruments panel. Hence, supporting information such as task needs to be displayed on a head-up display (HUD) or helmet-mounted display (HMD), or provided to the pilot by acoustic or haptic feedback.

Figure 9 – Pilot assistance for fighter air-to-air refuelling using HoloLens 2

The first step in this research involved interviews with fighter pilots to understand the challenges associated with air-to-air refuelling. The insights gained from these interviews guide a "Hierarchical Task Analysis (HTA)" to derive the key elements crucial for SA, known as "Situation Awareness Requirements (SAR)." Pilots rated these SARs based on relevance, allowing the most important parameters to be integrated into an assistance concept for air-to-air refuelling. The study interviewed 16 fighter pilots, including the Bundeswehr Technical Center for Aircraft and Aeronautical Equipment 61 (WTD 61), Tornado pilots and Eurofighter pilots from the German Air Force squadrons. The pilots ranged in age from 29 to 41 years and had between 300 and 3500 total flight hours, with experience flying various jets. During these interviews, pilots were asked about specific information needs, external references, and relevant parameters across the various phases of air-to-air refuelling: AAR Preparation, Pre-Contact, Establishing Contact, Maintaining Contact, and Disconnect. This approach provided comprehensive insights into the complexities of these phases, leading to a better understanding of

how to support pilot SA and improve performance during air-to-air refuelling. A key finding from this analysis is that fighter pilots use various optical references in their cockpits in conjunction with tanker references to facilitate AAR. These cockpit references, such as fixed markings on the HUD, the cockpit frame, or even the detonating cord on the canopy, are aligned with specific points on the tanker, like stripes, the refuelling pod, or other structural features. This alignment provides pilots with crucial guidance during AAR, improving accuracy and safety.

The interviews identified two strategies pilots use to establish contact during air-to-air refuelling. The first strategy is the straight approach, where pilots align the probe directly with the drogue, applying a single throttle input to make contact. This method aims to reduce the impact of the bow wave on the drogue's stability. The second strategy is the oblique approach. In this case, pilots start from a position slightly below and laterally offset from the drogue, then follow an oblique path to establish contact. This strategy is designed to anticipate and mitigate the bow wave's effect. Both approaches offer pilots options to adapt to varying conditions during refuelling.

These interviews were followed by a hierarchical task analysis in order to structure and fully understand the task of refuelling a fighter aircraft inflight using probe-and-drogue equipment from the receiver's perspective. A situational awareness requirements analysis, originally developed by Endsley, was then applied and enhanced regarding the air-to-air refuelling process[23]. The extracted requirements were then rated by the jet pilots regarding their relevance in the specific phases of the refuelling process. Based on these findings and with an understanding of the most critical parameters, several assistance systems were subsequently developed, with two of them integrated into the MARS-FIT simulator environment during the initial phase of expansion.

The holograms for these two assistance systems were implemented on the Microsoft HoloLens 2 mixed-reality device used as HMD and subsequently evaluated in a study focusing on human factors (see Figure 9). The first was an overtake speed scale, allowing pilots to precisely control their speed relative to the tanker, reducing the risk of rapid closure and enhancing safety during air-to-air refuelling [24]. In order to achieve a safe and reliable contact, this closure rate should stay best between 3 and 7 ft/sec during the contact establishment. The second system was a drogue highlighting system, designed to improve visibility of the refuelling drogue.

To assess the impact of these systems, evaluation tests were conducted in the fixed-base flight simulator MARS-FIT to measure fighter pilot workload with and without the assistance systems. The controlled environment allowed for direct comparison, providing quantitative data on the systems' effectiveness in reducing pilot workload and improving air-to-air refuelling operations. It acknowledges that SA and mental workload are not directly correlated, and reducing mental workload through increased SA depends on several factors, including the assistance system's design.

The human factors evaluation revealed that the success rate for making contact improved when the assistance system was active. Notably, the overtake speed assistance system demonstrated an enhancement in situational awareness (SA), and both assistance systems contributed to reducing pilot workload. The drogue highlighting system was found especially useful in low-light conditions, helping pilots locate the drogue quickly and reduce the chance of missed attempts. Overall, the pilots showed a positive reception toward the assistance systems used in aerial refuelling.

4.1.2 Pilot Assistance by modifying the flight control laws

Another way to support the pilot in the contact phase lies in the modification of the control laws. For the FMTA, two methods have been implemented and tested. In the first mode, the spoilers have been used in combination with other control surfaces to create direct-lift-control (DLC) behaviour that facilitates vertical control, similar to the *AAR Law* of the Airbus A400M. With the second method, called flight-path-vector (FPV) mode, the side stick inputs are translated into flight path angle and track offset commands that provide enhanced stability and allow smoother control of the relative position. Both control modes are still considered as pilot assistance (by opposition to automated modes), as they keep the pilot fully engaged and do not require additional sensors for the relative positions between receiver and tanker or probe and drogue.

The acceleration augmentation system (AAS) that was developed in F(AI)^{2}R for fighter refuelling

belongs to this category, too. As the precise and rapid control of the airspeed is one of the challenges for the pilots during AAR, the intent of the AAS is to provide the pilot with a more immediate and predictable control of the airspeed. In order to achieve this, the speed brake of the aircraft is used, benefiting from the direct influence on the drag and thus the airspeed. To make this possible, the speed brake starts out partially deflected, as soon as the AAS is engaged. This initial deflection allows the use of the speed brake for both acceleration and deceleration by either decreasing or increasing the deflection angle. When using the AAS, the delay to a throttle input caused by the engine spool up is compensated by a retraction of the speed brake. The resulting effect on the airspeed sets in almost immediately. As soon as the engine starts to increase its thrust, the speed brake extends again in order to restore the initial equilibrium. The result of the combined use of speed brake and engine is a hardly delayed constant acceleration. [19]
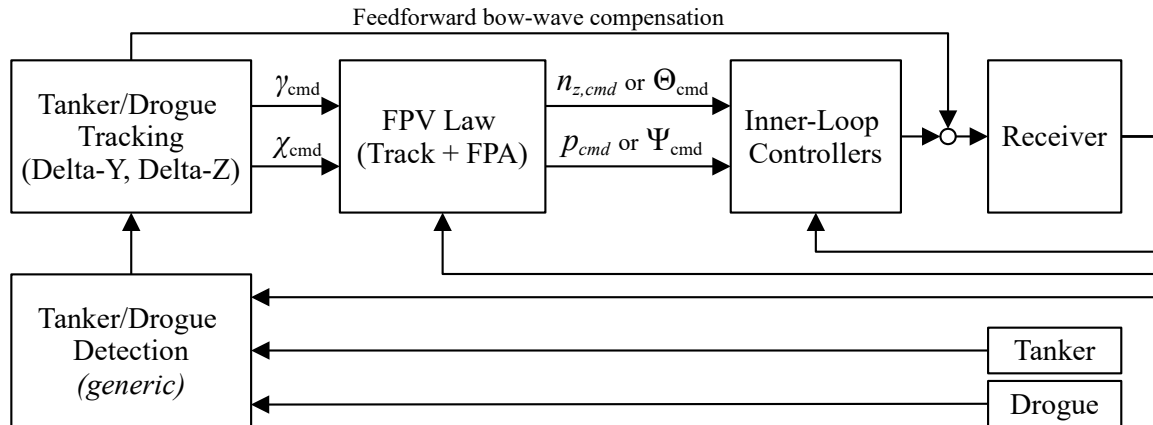
Figure 10 – Cascaded lateral/vertical control loops for assisted and automated air-to-air refueling (longitudinal/speed loop not represented)

4.2 Automation

Automation, in contrast to pilot assistance, is understood as the complete adoption of a task or control channel by the machine, whereas the pilot only commands the objective or setpoint, like for cruise control in a car. A similar concept, called speed hold controller (SHC), was implemented for the receiver. This concept is built around the AAS but additionally can acquire and hold the given overtake velocity by use of the combination of speed brake and engine. The pilot can input the commanded overtake velocity in steps of 0.5 kt. Since the pilots command the overtake velocity themselves, it is assumed that they can use this controller without the need to adapt their refuelling strategy. The advantages of this control concept are the guaranteed minimum overtake velocity needed for successful coupling, as well as no danger of accidentally exceeding the maximum limits. Additionally, after commanding the overtake velocity the pilot can direct his full attention on the stick inputs to track the basket. [19]

Conversely, to automatically adjust the relative position in lateral and vertical direction, other concepts have been investigated too. For the fighter as receiver, a position tracking controller (PTC), and for the FMTA as receiver, a similar drogue tracking controller (DTC) have been developed and implemented.

These controllers use the measured relative position between receiver and drogue to align the probe with the drogue during the approach and thereby enhance the probability for a successful contact.

The main idea of the PTC is to track the middle of the basket with the refuelling probe, by using the aileron and elevator, in the same way a pilot would carry out a manual contact. Due to the distance between centre of rotation and probe tip, the achievable bandwidth of the system is limited. During the final approach, the displacement of the drogue caused by the bow wave, as well as the resulting forces of the hose system lead to a very dynamic motion, that can't be tracked in a closed loop by the controller. Therefore, an additional offset to the real drogue position is added to the aim point that is based on the current relative velocity and position.

For the FMTA as receiver aircraft, the DTC has been implemented as an additional outer loop that calculates a track offset and an flight-path-angle (FPA) offset command for the respective inner loops of the autopilot in order to align the probe and the drogue. In contrast to the PTC of the fighter aircraft, the bow wave compensation in the DTC of the FMTA is implemented as a feed-forward controller that commands rotational rates to the inner loop of the flight control system. For this purpose, the predicted time to contact is used so that the influence of the closure rate is incorporated in the controller structure. The wind field of the bow wave is depending on the absolute airspeed of the receiver, thus the change of the wind field itself depending on the closure rate is negligible. However, the exposure time of the bow wave (i. e. the time during which the bow wave is effecting the refuelling drogue) is strongly influenced by the relative airspeed of the receiver towards the drogue, which is the closure rate. Because of this effect, a gain scheduling has been implemented to take into account that the exposure time of the bow wave is also a function of the closure rate.

As the receiver pilot remains in the loop for controlling the closure rate (either manually or by setting the speed setpoint of the autothrust), the implemented concepts are still considered as partial automation.

4.3 Evaluation in the Simulator with Pilots in the Loop

For the evaluation of the automation functions for the GFA, a simulator test campaign was carried out with test pilots of the German Air Force. One of the key elements of this campaign was an extensive familiarization phase to prevent distortion of the results due to training effects. As a next step a Handling Quality Assessment was carried out to evaluate the AAS and SHC outside of the scope of air-to-air refuelling. Finally, a set amount of operational contacts was performed for each of the automation functions. Additionally, manual contacts without automation were integrated into the test plans to provide a baseline for the subsequent comparisons. The whole test campaign was completed by surveys capturing the pilot comments regarding the automation functions. The general outcome of this test campaign was a high acceptance for automation functions to aid during air-to-air refuelling. Based on the pilot comments the main workload during air-to-air refuelling is focused on the control of the position and less on the control of the airspeed. As a consequence, the automation functions assisting in the control of the airspeed were rated as less helpful by the pilots. Suggested improvements for the PTC included more information displayed to the pilot, including a prediction, if the contact approach will be performed successfully, as well as an indication at which position the controller can be activated.

Simulator tests with different control modes and combinations have been conducted. The pilots showed high acceptance for the implemented assistance and automation concepts, and achieved significantly better contact success rates with such support. This encourages further development of the control laws in the coming follow-up project FARAO, where also the extension of the concepts to other refuelling phases will be pursued.

The assistance and automation functions for the FMTA as receiver aircraft have also been evaluated in a simulator campaign in the AVES simulator with six A400M pilots of the German Air Force. Figure 11 shows an example screenshot from the recorded video material in this campaign. In order to reduce the influence of training effects, not only an extensive familiarization phase was conducted but also the baseline configuration has been evaluated again after testing the various assistance and automation functions. In addition to that, many short breaks or longer breaks have been included in the schedule to reduce the influence of fatigue after a high number of simulator tests. A training effect has been identified indeed for each pilot during the numerous tests in the simulator, but the performance and success rate with the implemented assistance and automation function were still significantly better than when re-running the tests with the baseline configuration at the end of the day. The baseline configuration was defined as a configuration of the flight control laws similar to the *AAR Law* of the Airbus A400M, i. e. usage of the spoiler surfaces for direct lift control and a slight modification of the aircraft behaviour around the roll axis. The planning of the day included numerous breaks and also each block was performed successively by each of two pilots, so that fatigue of the pilots is not expected to have played a noticeable role.

Figure 11 – Simulator tests with FMTA as receiver in the AVES simulator with A400M pilots

In total, more than 400 coupling attemtps with manual flight control have been flown in the simulator during this campaign. Also, the simulator campaign included the evaluation of the newly implemented turbulence model that has been mentioned in section 2.2.3. The general feedback of the pilots about the assistance and automation functions was very positive and the significantly better performance and success rate also support the suggestion of a further investigation of these concepts. The turbulence model has been assessed as highly realistic and the feedback about the additional effects that have been modeled specifically for the simulation of air-to-air refuelling was very positive. The detailed evaluation of this simulator campaign is still ongoing and the results are planned to be published in a separate paper in the future.

4.4 Actively Controlled Drogue

Another technology which can contribute to ease establishing contact between probe and drogue is an actively controlled drogue. The idea is to control aerodynamic forces on the drogue to stabilise it (i.e. damp its motion) or to actively steer it towards the probe, whereby the latter concept has been named *smart drogue*. The actively controlled drogue, regardless whether just stabilised or actively steered, is also providing a noticeable compensation of the receiver bow wave. If connected to the drum mechanism, the smart drogue could even move towards the receiver, instead of the needing the receiver to accelerate and then decelerate again.

A simulation model of the smart drogue was developed based on wind tunnel test data (cf. section 5.2.1) and integrated into the full simulation. Two controllers were developed: one just adding damping to the hose and drogue motion and one also actively steering the drogue towards the probe. For the latter controller, the relative position and motion between the receiver probe and the drogue needs to be known: this modes assumes that they are measured or estimated.

The control authority with the aerodynamic surfaces is limited, the drogue can only move by about 1–1.5 m away from its natural equilibrium. For the smart drogue this already virtually increases the drogue size by a significant factor and makes it significantly easier for the receiver pilot to engage. Additionally, the smart drogue tends to fight the bow wave and so pilots do not need as large last minute corrections to successfully connect with the drogue. During early tests, it appears that having the smart drogue attempting to align in front of the probe was not desirable. It makes particularly hard for pilots to assess whether they are approaching the drogue around its natural equilibrium or whether they are already misaligned and potentially at the border of the control authority of the drogue. Pilots may better assess the situation in the lateral direction based on the angle between the drum and the hose, but is nearly impossible to assess in the vertical direction. As a consequence, the smart drogue position controller activates only in the last meters: pilots approach a stabilised/damped

drogue around its natural equilibrium position and only when attempting to establish contact the position controller activates and helps correcting any lateral of vertical offset between probe and drogue.

The tests performed with the A400M pilots in the FMTA-FMTA scenario were very positive. In particular, the combination of FPV law with smart drogue received extremely positive evaluations by the pilots, which was also confirmed by the objective evaluations of the success rate where this combination outperform the other modes. Pilots obviously felt very confident and started to be much more aggressive in their approach of the drogue, leading to much quicker contacts, but also some near miss that would certainly have been avoided if they had been approaching the drogue more prudently (as they certainly would in real conditions). Whilst the results were extremely positive, one should however keep in mind that judging distances (in all axes, but even more the depth than lateral and vertical offsets) is more difficult in the simulator than in real life. So the advantage of having a smart drogue, compared to a regular drogue, may in practice be lower than during these simulator tests. Refuelling drogues are also exposed to a very harsh environment and are regularly damaged and repaired: extreme robustness of the control system (actuators, surfaces) will be required. With this regard, the smart drogue technology is still at a relatively low technology readiness level (TRL 2-3).

5. Scaled Demonstrations

As shown in the previous sections, a large part of the F(AI)^{2}R project has focused on the modelling and simulation tools and on testing various concepts in simulator with pilots. Scaled demonstrations for specific components were also undertaken [25]. Two main systems were considered and tested: a relative navigation system between receiver, tanker, and drogue and a smart drogue. In both cases, the down-scaling brought additional difficulties and if later applied to large aircraft different solutions might be considered, but still interesting lessons can be learned at the considered scale. The work performed on both systems are described in the sections 5.2 and 5.2.1. Before that, the platforms used for these scaled demonstrations are presented in section 5.1.

5.1 Scaled Demonstration Platforms

As scaled flying demonstrators, two fixed wing UAVs were used and customised. They are depicted in Figure 12 on ground at the Experiment Test Center for Unmanned Aircraft Systems[2] in Cochstedt, Germany. For the tests the tanker demonstrator tows the scaled drogue with a cable (no real hose and no fuel transfer). The receiver demonstrator should fly in close formation, sense the relative position with respect to the tanker demonstrator and to the drogue demonstrator. For sake of readability, in the following the expressions tanker, receiver and drogue will be used for the scaled demonstrators.

The different control modes of the drogue (e.g. stabilisation, probe tracking) can also be tested. The towing cable can be released by a servomotor and a rescue parachute is deployed to allow the drogue to be quickly disconnected from the tanker in the event of a malfunction.

For the scaled demonstration, the tanker engine maximum power and the expected drag for the drogue itself impose a weight limit of 1.0 kg for the scaled drogue. The scaled drogue shape is based on a trailing cone with holes to achieve stable flight behaviour and simplify its construction. The holes mitigate the turbulence within the cone by allowing part of the flow energy to traverse the cone surface. This design similar to the some of the trailing cones used for pressure measurements. The usual spoke shape allows the drogue to fold itself in the pod but would have been more complex and too heavy to build in scaled version.

5.2 Relative Navigation Between Receiver, Tanker, and Drogue

The determination of the relative position between receiver and drogue is not trivial but essential for automated refuelling. Various sensors and systems were integrated on the tanker and receiver platforms to test their performance individually and once fusioned together.

A camera and a LiDAR sensor were installed in the receiver to capture the relative position and motion

---

[2]https://www.dlr.de/en/ux

Figure 12 – Receiver Demonstrator on the left & Tanker Demonstrator on the right [25]

of the drogue. The measurements were then fused with GNSS and IMU data and then transmitted to the drogue via data link. The smart drogue requires this information when in position tracking mode (see later in section 5.2.2).

The concept of operations foresees that the two aircraft first enter a formation based on their respective positions determined by applying a standard navigation Kalman filter to fusion Global Navigation Satellite System (GNSS) position and inertial sensors (IMU). The GNSS and inertial sensors as well as the navigation filter from the used Pixhawk 4 platform are used. The goal of GNSS-based formation is for the tanker to align its position and velocity with the receiver and form a formation between the two, with the tanker flying approximately 30 m ahead of the receiver. The assumed accuracy for this operation is about 1–5 m, depending on the external conditions of the environment.

Once the GNSS-based formation is established, the visual perception will take over the alignment process. It is envisioned that the visual perception sensors will be able to perform the localisation of the drogue with an accuracy of 0.5 m within a range up to 20 m . In the contact area (1 m in front of the sensors), an accuracy of less than 0.1 m is expected.

For this, a hardware and software setup based on two complementary sensors was developed. Both sensors monitor the same Field of View (FoV) with different measurement principles: the first is a camera and the second one a Light Detection and Ranging Sensor (LiDAR). The estimate are fused with the external global position provided by the autopilots of the drogue and the receiver. Figure 13 shows a schematic representation of this setup. The sensor outputs are processed individually and in parallel to cover the loss of a single lane. Finally, the three lanes (camera, LiDAR, and autopilot alignment) are competitively fused to provide the result to the drogue controller described later in section 5.2.2.

In the visual approach, the two optical sensors operate in the near-infrared (NIR) range and provide a relative position estimate between the drogue and the receiver in real time. This redundancy ensures that the maneuver can be performed even if one sensor is unavailable. The use of NIR light has the advantage of being less susceptible to background noise in the image, primarily because light coming from the sun in the NIR band is blocked in the upper layers of the atmosphere. The camera perception uses a tracking of active markers: the inside of the drogue cone is equipped with seven NIR LEDs arranged in a specific pattern and eventually a Perspective-n-Point (PnP) algorithm is used to estimate the full pose of the drogue with respect to the receiver-mounted cameras.

The LiDAR system used is a three-dimensional laser scanner that takes multiple distance measurements to create a three-dimensional image of the environment. Two perception approaches to estimate the drogue position. The first relies on the fact that only a few objects (tanker, receiver, and drogue) are in the LiDAR range during the refuelling maneuver. Besides, because of their clear spatial distribution, spatial segmentation of the measurements should be easy. After clustering the
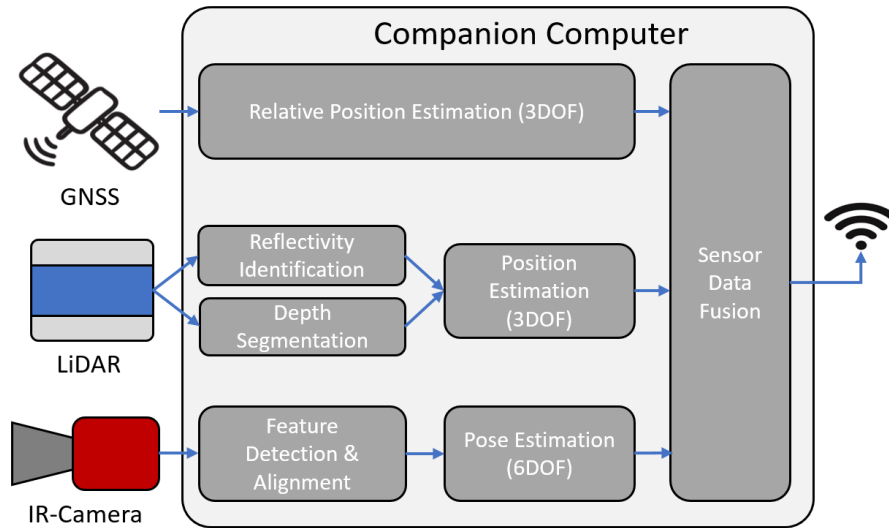
Figure 13 – Overview of the perception concept [25]

LiDAR measurements, three clusters representing the three objects eventually remain. Knowledge of the formation structure allows excluding the clusters representing the tanker and receiver to obtain the measurements corresponding to the drogue.

For simplicity in the envisioned tests, a second approach based on ensuring unique NIR properties for the drogue was used. A microprism coating was applied to the inside of the cone. This coating reflects the incident light back in the same direction from which it came, acting like a passive reflector familiar from traffic signs. With this setup, the cone is the brightest object in the LiDAR point cloud and can easily be identified.

In parallel with the processing of the reflectivity data, the distance data are also processed to achieve a segmentation based on a distance separator. For this purpose, an approach is implemented in which the depth difference between neighboring measurements is validated by a threshold value corresponding to the size of the drogue.

Finally, the results of both processing steps (reflectivity-based and distance-based) are combined to find intersections that have the highest probability of being the drogue.

5.2.1 Wind Tunnel Testing

To obtain valid aerodynamic data for the drogue, including with the control surfaces effectiveness and their impact of the cone in their wake, wind tunnel tests were performed in the DNW-NWB tunnel from DLR Braunschweig. Figure 14a shows a picture of one such test with a deflected control surface in the front. The data obtained supported the modelling of the drogue for the investigation made in simulation mentioned above and also the tuning of the controllers for the scaled free-flying experiment.

5.2.2 Free-Flying Experiments

For the scaled-testing of the smart drogue concept, a smart drogue demonstrator was defined with a scale compatible with the test platforms used and shown in section 5.1. A control segment containing sensors, controllers, and servomotors is added in front of the drogue cone to provide control of the vertical and lateral motions. The servomotors move four control surfaces, equally distributed around the symmetry axis of the control segment. The aerodynamic forces and moments generated by these surfaces permit to control the drogue. This modular structure shall permit to quickly modify some of the components (e.g. use larger control surface, a different avionics casing), without having to redesign the entire system. Figure 14b shows the drogue's main components: the fuselage, the trailing cone, and the control surfaces. The length of the drogue is approximately 450 mm and the cone bottom has a diameter of 370 mm. The area of the control surfaces is 0.012 m^2 with a maximum

(a) During wind tunnel tests

(b) Scaled Drogue Demonstrator used in flight experiments [25]
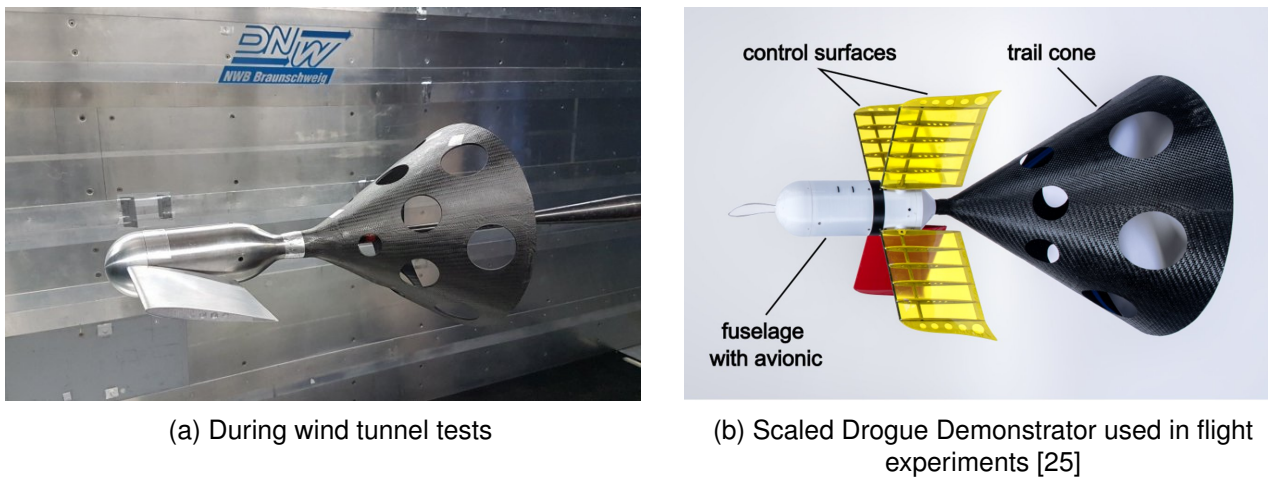
Figure 14 – Steerable drogue variants used during the tests

deflection of ±4 deg. They are directly mounted to the servomotors, which makes the assembly very compact but limits the maximum hinge moment.

The tanker fuselage carries the avionics, consisting of the autopilot, the GNSS antenna and two telemetry units with antennas, the servomotors, and the power supply. The autopilot hardware is a commercial off-the-shelf (COTS) Pixhawk. DLR has regularly used these platforms in various of its UAV research projects and has therefore significant experience with them. A dedicated toolchain, supporting the controller code generation via Simulink and the Embedded Coder.

The drogue controller has been divided into modes that are used in parallel. This allows the effects to be switched on and off quickly according to need and effectiveness. The various modes are presented below in brief descriptions. The modes are then summed and the resulting commands are limited in terms of maximum deflections.

The first mode, a manual control with roll-angle mixing, allows a human operator to reduce offsets orthogonal to the direction of flight to position the drogue relatively to the receiver. This human operator is needed for a first testing of the capabilities to manipulate the position. The roll-angle mixing ensures that the human operator can control lateral of vertical commands without caring about the current bank angle of the drogue. In the second mode the drogue is stabilised in the roll axis with a PI inner-loop on the roll rate and an bank angle outer-loop.

The third and last mode is the position control mode. In this mode the feedback input for this control algorithm is the sensor data provided via the data link to the receiver. Two PID controllers are used for controlling the later and vertical position of the drogue, such that the drogue aligns perfectly with the receiver probe. These controllers are gain-scheduled with airspeed and contain various protection/non-linearities (e.g. saturations, anti-windup). If the drogue offsets with respect to the receiver probe are stable and sufficiently small the tanker winch can automatically unroll the cable to reduce the longitudinal offset.

Due to series of issues with the test platforms, the test have been delayed. Only partial/component tests could be made until now. Some of the controls were tested in driving test (towing the drogue behind a ground vehicle). The complete scaled flight demonstration is still planned for the near future.

6. Conclusion

The paper gives an overview about the research progress at the DLR in the area of simulation and automation of air-to-air refuelling. The approach started from the simulation of the refuelling formation, to understand the flight physics and include the relevant aspects into the models. For automation, the focus was first on how to facilitate the coupling process for the manned receiver by pilot assistance, and then step-wise extend the capabilities of the automation.

Many milestones have been achieved so far, but there is still a way to go until the concepts are

mature enough for the implementation into real aircraft and future UAVs. For this reason, a follow-on project FARAO was initiated to further improve the automation concepts and evaluate them with the support of military pilots in the DLR simulator facilities. Eventually, the transfer of the technology to actual assets is only possible in cooperation with the industry. Under the umbrella of the European Defence Agency (EDA) this process has been recently started within a project on Automated Air-to-Air Refuelling for Hose and Drogue Systems (A3RHD).

7. Acknowledgements

8. Contact Author Email Address

mailto: thomas.jann@dlr.de

9. Copyright Statement

References

[1] N. Fezans and T. Jann. Modeling and simulation for the automation of aerial refueling of military transport aircraft with the probe-and-drogue system. In *Proc. of the AIAA AVIATION 2017 Modeling and Simulation Technologies Conference*, number AIAA 2017-4008, Denver, CO, USA, June 2017. doi: 10.2514/6.2017-4008.

[2] N. Fezans and T. Jann. Towards automation of aerial refuelling menoeuvres with the probe-and-drogue system: modeling and simulations. *Transportation Research Procedia*, 29:116–134, 2018. doi: 10.1016/j.trpro.2018.02.011.

[3] P. Ohme. A model-based approach to aircraft takeoff and landing performance assessment. In *Proceedings of the AIAA Atmospheric Flight Mechanics Conference and Exhibit*, Chicago, IL, USA, Aug. 2009. AIAA 2009-6154. doi: 10.2514/6.2009-6154.

[4] T. Jann. Coupled simulation of cargo airdrop from a generic military transport aircraft. In *Proceedings of the AIAA Aerodynamic Decelerator System Technology Conference*, Dublin, Ireland, May 2011. AIAA 2011-2566. doi: 10.2514/6.2011-2566.

[5] S. Geisbauer, N. Schade, S. Enk, H. Schmidt, and J. Arnold. Experimental and numerical investigation of the flow topology during airdrop operations. In *Proceedings of the AIAA Aerodynamic Decelerator System Technology Conference*, Dublin, Ireland, May 2011. AIAA 2011-2565. doi: 10.2514/6.2011-2565.

[6] S. Geisbauer and H. Schmidt. Development and validation of a RANS-based airdrop simulation approach. In *Proc. of the 33rd AIAA Applied Aerodynamics Conference*, Dallas, TX, USA, 22-26 June 2015. AIAA 2015-3016. doi: 10.2514/6.2015-3016.

[7] H. Schmidt. Implementierung eines MKS-fahrwerksmodells in Matlab/Simulink mittels „response surfaces". Technical report, DLR (German Aerospace Center) - Institute of Aeroelasticity, 2012. Internal report - IB 232-2013 C 03.

[8] S. Geisbauer. Untersuchung des Einflusses generischer Vorderkantenbeschädigungen auf die aerodynamische Leistungsfähigkeit von Flugzeugprofilen. Technical report, DLR (German Aerospace Center) - Institute of Aerodynamics and Flow Technology, 2012. Internal report - IB 124-2012/903.

[9] H. Duda, T. Gerlach, S. Advani, and M. Potter. Design of the DLR AVES research flight simulator. In *Proc. of the 2013 AIAA Modeling and Simulation Technologies Conference*, pages 1–14, Boston, MA, USA, 19-22 August 2013. AIAA 2013-4737. doi:10.2514/6.2013-4737.

[10] N. Fezans and A. Koloschin. Extending Simulink with blocks managing complex objects collaboratively – Application to air-to-air refueling simulation. In *Proc. of the 2022 AIAA SciTech Forum*, San Diego, CA, USA and online, 3-7 January 2022. AIAA 2022-0808. doi:10.2514/6.2022-0808.

[11] S. O. Schmidt, Jones M., and P. Löchert. Evaluation of a real-time simulation environment for helicopter air-to-air refuelling investigations. *The Aeronautical Journal*, 127(1311):754–772, May 2023. doi:10.1017/aer.2022.106.

[12] P. Löchert, S. O. Schmidt, T. Jann, and Jones M. Consideration of tanker's wake flow for helicopter air-to-air refueling. In *Proc. of the 2021 AIAA Aviation Forum*, online, 2021. AIAA 2021-2561. doi:10.2514/6.2021-2561.

[13] L. T. Nguyen, M. E. Ogburn, W. P. Gilbert, K. S. Kibler, P. W. Brown, and P. L. Deal. Simulator study of stall/post-stall characteristics of a fighter airplane with relaxed longitudinal static stability. In *NASA Technical Paper 1538*, December 1979.

[14] J. Gotschlich and M. Jones. Online trimming of flight dynamics models using the 2simulate realtime simulation framework. In *Proc. of the 2018 AIAA SciTech Forum*, Orlando, FL, USA, January 2018. AIAA 2018-0120. doi:10.2514/6.2018-0120.

[15] César González Gómez. Helicopter aerial refuelling: A400m challenges. In *Society of Flight Test Engineers (SFTE) European Chapter*, 2022.

[16] X. Dai, Z. Wei, and Q. Quan. Modeling and simulation of bow wave effect in probe and drogue aerial refueling. *Chinese Journal of Aeronautics*, 29(2):448–461, Apr. 2016. doi:10.1016/j.cja.2016.02.001.

[17] M.-J. Maibach, M. Jones, and A. Strbac. Development of a simulation environment for maritime rotorcraft research applications. In *Proc. of Deutscher Luft- und Raumfahrtkongress (DLRK)*, Virtual, 2020.

[18] S. O. Schmidt, D. Greiwe, and T. Jusko. Pilot's gaze behavior during simulated helicopter air-to-air refueling. In *Proc. of the VFS 80th Annual Forum & Technology Display*, Montréal, Canada, May 2024. doi:10.4050/F-0080-2024-1294.

[19] P. Weber and P. Link. Simulator testing of semi-automated control concepts for the receiver aircraft during air-to-air refuelling with probe-and-drogue systems. In *Proc. of the 33rd Symposium of the SFTE European Chapter*, Nuremberg, Germany, May 2022.

[20] P. Perfect, E. Timson, M. D. White, G. D. Padfield, R. Erdos, and A. W. Gubbels. A rating scale for the subjective assessment of simulation fidelity. *The Aeronautical Journal*, 118(1206):953–974, Aug. 2014. doi:10.1017/S0001924000009635.

[21] L. L. Ngoc. *Augmenting Low-Fidelity Flight Simulation Training Devices via Amplified Head Rotations*. PhD thesis, Loughborough University, 2013. `https://hdl.handle.net/2134/14441`.

[22] M. R. Endsley. A survey of situation awareness requirements in air-to-air combat fighters. In *The International Journal of Aviation Psychology*, 1993.

[23] W. M. Jones A. H. Midkiff M. R. Endsley, T. C. Farley and J. R. Hansman. Situation awareness information requirements for commercial airline pilots. In *International Center for Air Transportation*, 1998.

[24] J. Schmelz, J. Lachmann, J. Ament, and L. Wandrey. Design and assessment of fighter pilot assistance systems for air-to-sir refuelling with probe-and-drogue-equipment. In *Proc. of the 33rd Symposium of the SFTE European Chapter*, Nuremberg, Germany, May 2022.

[25] Stefan Krause, Alexander Funke, and Sebastian Cain. Overview of a planned subscale in-air capturing demonstration. In *2024 IEEE Aerospace Conference*, pages 1–15, 2024. doi:10.1109/AERO58975.2024.10521033.